MICROBIOLOGY

RESEARCH ARTICLE

Jiang *et al.*, *Microbiology* 2017;163:1–15
DOI 10.1099/mic.0.000427

MICROBIOLOGY SOCIETY

The function of the three phosphoribosyl pyrophosphate synthetase (Prs) genes in hyphal growth and conidiation in *Aspergillus nidulans*

Ping Jiang,[1]† Wen-fan Wei,[1]† Guo-wei Zhong,[2] Xiao-gang Zhou,[1] Wei-ran Qiao,[1] Reinhard Fisher[3] and Ling Lu[1,*]

Abstract

Phosphoribosyl pyrophosphate synthetase, which is encoded by the Prs gene, catalyses the reaction of ribose-5-phosphate and adenine ribonucleotide triphosphate (ATP) and has central importance in cellular metabolism. However, knowledge about how Prs family members function and contribute to total 5-phosphoribosyl-α-1-pyrophosphate (PRPP) synthetase activity is limited. In this study, we identified that the filamentous fungus *Aspergillus nidulans* genome contains three PRPP synthase-homologous genes (*AnprsA*, *AnprsB* and *AnprsC*), among which *AnprsB* and *AnprsC* but not *AnprsA* are auxotrophic genes. Transcriptional expression profiles revealed that the mRNA levels of *AnprsA*, *AnprsB* and *AnprsC* are dynamic during germination, hyphal growth and sporulation and that they all showed abundant expression during the vigorous hyphal growth time point. Inhibiting the expression of *AnprsB* or *AnprsC* in conditional strains produced more effects on the total PRPP synthetase activity than did inhibiting *AnprsA*, thus indicating that different AnPrs proteins are unequal in their contributions to Prs enzyme activity. In addition, the constitutive overexpression of *AnprsA* or *AnprsC* could significantly rescue the defective phenotype of the *AnprsB*-absent strain, suggesting that the function of *AnprsB* is not a specific consequence of this auxotrophic gene but instead comes from the contribution of Prs proteins to PRPP synthetase activity.

INTRODUCTION

Phosphoribosyl pyrophosphate synthetase (Prs – EC: 2.7.6.1) catalyses the reaction of ATP to form 5-phosphoribosyl-α-1-pyrophosphate (PRPP) and AMP [1–5]. It has been identified that the Prs reaction product, PRPP, is involved in many different pathways, such as the pentose phosphate pathway and the *de novo* and salvage purine and pyrimidine nucleotide pathways, and in the biosynthesis of nucleotide coenzymes, histidine and tryptophan [2, 6–8]. Therefore, this information indicates the central importance of Prs enzymes in cellular metabolism.

Prs genes and their products are of interest not only for their importance to our understanding of biochemistry but also for their medical significance. In *Homo sapiens*, there are three Prs genes (*PRPS1*, *PRPS2* and *PRPS1L1*) whose superactivity is connected to gouty arthritis and whose diminished activity is associated with various neuropathies [9–13]. In addition, the missense mutations of PRPS1 result in Charcot-Marie-Tooth disease type 5 (or Rosenberg Chutorian Syndrome), Arts syndrome, PRS-I superactivity and X-linked nonsyndromic sensorineural deafness [10–12, 14–16]. In prokaryotes, Prs genes have been found and sequenced from a variety of bacteria; for example, the genome of *Mycobacterium tuberculosis*, which is the main pathogen of tuberculosis, contains a single Prs-encoding gene, *Mt-prs* (Rv1017c) [6, 17, 18]. Because PRPP is required for the cell wall biosynthetic precursor decaprenol-1-monophosphoarabinose to maintain cell integrity, this *Mt-prs* gene has been used as a potential drug target. In contrast, several isoforms of Prs have been cloned and described in plants, such as *Arabidopsis thaliana* and *Spinacia oleracea*, which have five and four Prs genes, respectively, and are located in different cellular organelles [3, 19, 20]. Similar to the eukaryotic system, most fungi also possess multiple Prs genes. For instance, in the filamentous hemiascomycete *Ashbya gossypii,* PRPP synthetase encoded by four genes (*Aer083cp*, *Agl080cp*, *Agr371cp* and *Adr314cp*)

Received 21 June 2016; Accepted 11 January 2017
Author affiliations: [1]Jiangsu Key Laboratory for Microbes and Functional Genomics, Jiangsu Engineering and Technology Research Center for Microbiology, College of Life Sciences, Nanjing Normal University, Nanjing 210023, PR China; [2]Department of Hygiene Analysis and Detection, School of Public Health, Nanjing Medical University, Nanjing 211166, PR China; [3]Department of Microbiology, Karlsruhe Institute of Technology (KIT) - South Campus Institute for Applied Biosciences, Karlsruhe, Germany.
***Correspondence:** Ling Lu, linglu@njnu.edu.cn
Keywords: phosphoribosyl pyrophosphate synthetase; *Aspergillus nidulans*; hyphal growth; conidiation.
Abbreviations: PRPP, 5-phosphoribosyl-α-1-pyrophosphate; RT-PCR, reverse transcription PCR; SIN, septum initiation network; aa, amino acids.
†These authors contributed equally to this work.
Eight supplementary figures are available with the online Supplementary Material.

plays important roles in cell growth and riboflavin production [21]. In comparison, the single cell yeast *Saccharomyces cerevisiae* is equipped with a set of five unlinked Prs genes (*ScPRS1–ScPRS5*). Deletion of any single or specific double combinations of *ScPRS* genes did not cause a lethal phenotype, indicating that some of the *ScPRS* genes are redundant. Moreover, genetic analysis and enzyme activity detection suggest that there existed more than one minimal functional unit capable of synthesizing phosphoribosyl pyrophosphate in *S. cerevisiae* [20, 22–28]. These results also suggest that Prs may have their own working paradigms in different species.

In our previous study, we found that there are three putative annotated genes (*AnprsA*, *AnprsB* and *AnprsC*) encoding PRPP synthetase in *Aspergillus nidulans*, according to the *Aspergillus* genome database (www.aspgd.org/). Moreover, we identified the AnPrs family as a suppressor of the septum initiation network (SIN) and that it acts antagonistically against SepH, a main component of SIN, so the down-regulation of the AnPrs family can bypass the requirements for SIN in septum formation and conidiation [29]. However, knowledge about how AnPrs family members work together and contribute to total PRPP synthetase activity is limited. In this study, we used constructed deletion and conditional strains for three *Anprs* genes to identify that *AnprsB* and *AnprsC* are auxotrophic genes, i.e. either deletion of *AnprsB* or *AnprsC* confers auxotrophic requirement for the downstream product of PRPP. In comparison, *AnprsA* is a non-auxotrophic gene. Moreover, we found that these three genes have different expression profiles at different developmental stages. The important functions of *AnprsB* and *AnprsC* are not irreplaceable but are mainly due to the contribution of Prs proteins to PRPP synthetase activity.

METHODS

Strains, media, culture conditions, plasmids and transformation

A list of *Asp. nidulans* strains used in this study is provided in supporting Table 1. The media YAG (yeast + agar + glucose media), YUU (YAG + uridine + uracil), MMPGRUU (MM + pyridoxine + glycerol + riboflavin + uridine + uracil), MMPDR (MM + pyridoxine + glucose + riboflavin), MMPDRUU (MM + pyridoxine + glucose + riboflavin + uridine + uracil) and MMDRUU (MM + glucose + riboflavin + uridine + uracil) and the Prs rescued medium MMR (MM + pyridoxine + glucose + riboflavin + uridine + uracil + adenine + guanine + histidine + tryptophan + AMP) as well as the concentration of the relative components are referred from previous references [29–35]. Growth conditions and derepression conditions for *alcA(p)*-driven expression were as previously described [36]. Expression of tagged genes under the control of the *alcA* promoter was regulated by different carbon sources: derepressing on glycerol and repression on glucose. Standard DNA transformation procedures were used for *Asp. nidulans* [37, 38].

Constructions of gene replacement strains

A strain containing the *AnprsB*-null mutation was created by double joint PCR [39]. The *Aspergillus fumigatus pyrG* gene in plasmid pXDRFP4 and the *Asp. nidulans pyroA* gene in plasmid pQa-pyro were used as selectable nutritional markers for fungal transformation, respectively. The linearized DNA fragment 1 which included a sequence of about 686 bp that corresponded to the regions immediately upstream of the *AnprsB* start codon was amplified with the primers Δ*AnprsB*-p1 and Δ*AnprsB*-p3 (Table 2). Linearized DNA fragment 2 including a sequence of about 541 bp that corresponded to the regions immediately downstream of the *AnprsB* stop codon was amplified with primers Δ*AnprsB*-p4 and Δ*AnprsB*-p6 (Table 2). Lastly, purified linearized DNA fragments 1 and 2 plus the *pyrG* gene or *pyroA* gene were mixed and used in a fusion PCR with primers Δ*AnprsB*-p2 and Δ*AnprsB*-p5. The final fusion PCR products were purified and used to transform *Asp. nidulans* strains TN02A7. A diagnostic PCR assay was performed to identify the deletion of the *AnprsB* gene by primers Δ*AnprsB*-p1 and Diag-*AfpyrG*-3′ (Diag-*AnpyroA*-3′). The *AnprsA* and *AnprsC* deletion transformants with the marker of *AnpyrG* and *AnpyroA* were constructed by using a similar strategy and transformed to TN02A7. To further identify auxotrophic requirements of *AnprsB* and *AnprsC*, conidia from the Δ*AnprsB* and Δ*AnprsC* heterokaryotic transformants selected by *AnpyroA* were inoculated into the selection medium MMDRUU supplemented with the predicted downstream products (uracil/uridine, adenine, guanine, histidine, tryptophan and AMP). Oligonucleotides used in this study are listed in Table 2.

Tagging of AnPrsA, AnPrsB and AnPrsC with GFP

To generate an *alcA(p)-gfp-AnprsB* fusion construct, a 909 bp fragment of *AnprsB* was amplified from TN02A7 genomic DNA with primer *AnprsB*-5′ (*Not*I site included) and primer *AnprsB*-3′ (*Xba*I site included) (Table 2). The 909 bp amplified DNA fragment was cloned into the corresponding sites of pLB01, yielding pLB-*AnprsB*-5′ [40]. This plasmid was transformed into TN02A7. Homologous recombination of this plasmid into the *AnprsB* locus should result in an N-terminal GFP fusion of the entire *AnprsB* gene under control of the *alcA* promoter and a fragment of *AnprsB* under its own promoter. The transformants, which were able to form the normal colony under the derepressing condition but could not grow under the repressing condition, was subjected to PCR analysis using a forward primer (GFP-5′) designed to recognize the *gfp* sequence and a reverse primer (*prsB*-3′) designed to recognize the *AnprsB*-3′ sequence. We used the similar way tagging of AnPrsA and AnPrsC with GFP.

Test transformants for heterokaryon formation

To detect if the primary transformants in Δ*AnprsB* and Δ*AnprsC* are heterokaryons, conidia from the surface of each of eight colonies (to avoid conidiophores as much as possible, as these multinucleated structures could allow the re-growth of the heterokaryon) were removed to the

Table 1. *Aspergillus nidulans* strains used in this study

Strain	Genotype	Source
TN02A7	*pyrG89; pyroA4,nkuA::argB; riboB2,veA1*	[55]
WJA01	*pyroA4; nkuA::argB2; riboB2; veA1*	[43]
ZGA01	*alcA(p)::GFP-AnprsA::pyr4; pyrG89; pyroA4; nkuA::argB; riboB2,veA1*	[29]
ZGA02	*ΔAnprsA::pyrG; pyrG89; pyroA4; nkuA::argB; riboB2,veA1*	[29]
WFA01	*ΔAnprsB::pyrG; pyrG89; pyroA4; nkuA::argB; riboB2,veA1*	This study
WFA02	*ΔAnprsC::pyrG; pyrG89; pyroA4; nkuA::argB; riboB2,veA1*	This study
WFA03	*alcA(p)::GFP-AnprsB::pyr4; pyrG89; pyroA4; nkuA::argB; riboB2,veA1*	This study
WFA04	*alcA(p)::GFP-AnprsC::pyr4; pyrG89; pyroA4; nkuA::argB; riboB2,veA1*	This study
WFA05	*gpd(p)::AnprsA::pyroA4; pyrG89; nkuA::argB; riboB2,veA1*	This study
WFA06	*gpd(p)::AnprsB::pyroA4; pyrG89; nkuA::argB; riboB2,veA1*	This study
WFA07	*gpd(p)::AnprsC::pyroA4; pyrG89; nkuA::argB; riboB2,veA1*	This study
WFA08	*ΔAnprsA::pyroA; pyrG89; nkuA::argB; pyroA4; riboB2,veA1*	This study
WFA09	*ΔAnprsB::pyroA; pyrG89; nkuA::argB; pyroA4; riboB2,veA1*	This study
WFA10	*ΔAnprsC::pyroA; pyrG89; nkuA::argB; pyroA4; riboB2,veA1*	This study

selective medium YAG and the non-selective medium YUU, respectively, using toothpicks that had been sterilized and then selected conidia were incubated at 37 °C for 48 h. After incubation, the growth phenotype of inoculated conidia on a solid plate had been examined [41]. If the deleted gene is essential or auxotrophic, then the null allele will be rescued by formation of a heterokaryon containing *pyrG*$^{-}$/*geneX*$^{+}$ nuclei and *pyrG*$^{+}$/*geneX*$^{-}$nuclei in a common cytoplasm. These nuclei are segregated into individual conidia during asexual spore formation, forming a mixture of *pyrG*$^{-}$/*geneX*$^{+}$ and *pyrG*$^{+}$/*geneX*$^{-}$ conidia on the surface of heterokaryon colonies. When this mixture is streaked on the YAG plate, the *pyrG*$^{-}$/*geneX*$^{+}$ conidia cannot grow because they are *pyrG*$^{-}$ and the *pyrG*$^{+}$/*geneX*$^{-}$ conidia cannot form colonies because they lack essential or auxotrophic *geneX* function. Thus, no colonies are formed on the YAG streaked plates if the original colony is a heterokaryon in which a null allele of an essential or auxotrophic gene is rescued. When streaked on the YUU non-selective plates, the *pyrG*$^{+}$/*geneX*$^{-}$ conidia still cannot grow due to lack of *geneX* function. However, the *pyrG*$^{-}$/*geneX*$^{+}$ conidia can grow because the *pyrG*$^{-}$ marker is complemented by the uridine and uracil in the YUU medium and these conidia have *geneX* function. The *pyrG*$^{-}$/*geneX*$^{+}$ conidia therefore germinate and grow to form colonies on the YUU medium. A similar strategy was used to identify the *AnprsB* and *AnprsC* deletion transformants with *AnpyroA* marker formed heterokaryon.

Microscopy and image processing

Several sterile glass coverslips were placed on the bottom of Petri dishes and gently overlaid with 1 ml liquid media containing conidia at 6×10^{7} ml^{-1}. Strains were grown on the coverslips at 37 °C prior to observation under a microscope. The GFP-AnPrsB and GFP-AnPrsC signals were observed in live cells by placing the cover slips on a glass slide. DNA was stained using DAPI (Sigma Aldrich, St. Louis, MO) after the cells had been fixed with 4.00 % paraformaldehyde (Polyscience, Warrington, PA) [42]. Differential interference contrast images of the cells were collected with a Zeiss Axio Imager A1 microscope (Zeiss, Jena, Germany). These images were then collected and analysed using a Sensicam QE cooled digital camera system (Cooke Corporation, Germany) with the MetaMorph/MetaFluor combination software package (Universal Imaging, West Chester, PA), and the results were assembled in Adobe Photoshop 7.0 (Adobe, San Jose, CA).

Western blotting analysis

For immunodetection, conidia at 1×10^{7} conidia ml^{-1} of *alcA(p)-gfp-AnprsA*, *alcA(p)-gfp-AnprsB* and *alcA(p)-gfp-AnprsC* were grown in 100 ml liquid medium of MMPGRUU and MMPDRUU, respectively, then incubated on a rotary shaker (QHZ-123B,Taihua CO.) at 220 r.p.m. at 37 °C for 18 h. Each mycelium was filtered through cheese cloth, moisture was blotted with filter paper and the mycelium was ground in liquid nitrogen. Then, 1 g of the well-ground fungi powder was placed into a small lysis tube by adding an appropriate amount of ceramic beads and then lysed with RIPA buffer containing 50 mM HEPES (pH 7.4), 137 mM KCl, 10.00 % glycerol, 1 mM EDTA, 1 µl ml^{-1} pepstatin A, 1 µl ml^{-1} leupeptin, 1 % Triton X-100, 0.10 % SDS, 1.00 % deoxycholate and 1 mM PMSF for 30 s on ice. The lysed solution was centrifuged at 12 000 r.p.m. for 15 min at 4 °C, and the supernatant was collected for Western blotting assay. For the quantification of the protein concentration, a BSA protein assay kit (Beyotime P0012, China) was used as a standard according to the manufacturer's protocol. Finally, aliquots (40 µg for total protein) of cell lysates were separated on 10.00 % SDS-PAGE, and immunoblotting was performed as described previously with GFP antibody (1 : 1000, Roche Applied Science) and anti-mouse IgG conjugated to alkaline phosphatase (1 : 2000, Vector laboratories 94010, Burlingame, CA). The protein bands were stained by using an NBT/BCIP alkaline phosphatase colour development kit (Beyotime

Table 2. Primers used in this study

Primer name	DNA sequence 5′–3′
Δ*AnprsA*-p1	ATCATCCAGAGCGGCAGCGAGAA
Δ*AnprsA*-p2	GTCACGTTCTCGGAATTCTTGT
Δ*AnprsA*-p3	CTATTATCTGACTTACCCCAAGACGAGGTGACC TTGTACGAGCC
Δ*AnprsA*-p4	CCAAGAGAAAGCGTCAAGTCAGCAATAGCGAC TGGGCTGTGTG
Δ*AnprsA*-p5	GATACTTCAGATTTCACCGTCC
Δ*AnprsA*-p6	CAACGGGTACGGGTAACGGTCAG
Δ*AnprsB*-p1	GAAGGTATGAATGGCGTGAG
Δ*AnprsB*-p2	CGCGTAGTATATCAGCTAATCC
Δ*AnprsB*-p3	CTCTAGATGCATGCTCGAGC AGGGCGAGG-GAAACTAAA
Δ*AnprsB*-p4	CAGTGCCTCCTCTCAGACAG CGTCCTCATG TGGGGTTT
Δ*AnprsB*-p5	TACAAGAGACATGGTCTGTCCA
Δ*AnprsB*-p6	TATTCCGCCAGACAAAGC
Δ*AnprsC*-p1	CTATTGGGAACTTATCGC
Δ*AnprsC*-p2	TCGTGTATGATGGGAAAT
Δ*AnprsC*-p3	GGAGCAAAGCAGGAGAAT CCTTTCTTAG TGGACCTTG
Δ*AnprsC*-p4	TCTTGGCTCTATCGTATTCTT AGCCTTCCATC TACCATA
Δ*AnprsC*-p5	ATAGGCGTTTGGAGTTTT
Δ*AnprsC*-p6	TGAGTTCGTTTAGCCTGT
pyrG-Forward	GCTCGAGCATGCATCTAGAG
pyrG-Reverse	GATACAGGTCTCGGTCCCTA
AnpyroA-Forward	TTGGCGGGTAAGTCAGATAATAG
AnpyroA-Reverse	CTGACTTGAC GCTTTCTCTT GG
Δ*AnprsA-1*-p3	CTATTATCTGACTTACCCGCCAAGACGAGG TGACCTTGTACGAGCC
Δ*AnprsA-1*-p4	CCAAGAGAAAGCGTCAAGTCAGCAATAGCGAC TGGGCTGTGTGC
Δ*AnprsB-1*-p3	CTATTATCTGACTTACCCGCCAAAGGGCGAGG-GAAACTAAA
Δ*AnprsB-1*-p4	CCAAGAGAAAGCGTCAAGTCAGCGTCCTCATG TGGGGTTT
Δ*AnprsC-1*-p3	CTATTATCTGACTTACCCGCCAACCTTTCTTAG TGGACCTTG
Δ*AnprsC-1*-p4	CCAAGAGAAAGCGTCAAGTCAGAGCCTTCCA TCTACCATA
Diag-*AnpyroA*-3	ATTAGCATTCCGCTTCTTCC
Diag-*AfpyrG*-3′	GATACAGGTCTCGGTCCCTA
AnprsB-5′	TGCTCTAGAAAGTGTTCCGCATGTATC
AnprsB-3′	ATAAATATGCGGCCGCTGGCGACGAATTCTATC
AnprsC-5′	AAATATGCGGCCGCTGGTTCGAAATATCGTCG TC
AnprsC-3′	TGCTCTAGAGCAAGATCGTCAATCAGG
GFP-5′	GACACCCTCGTCAACAGGATCG
prsA-5′	CATGCGTCAACAGTGTTGC
prsA-3′	GAAAGGCTCGGCGAATAGGTTGT
prsB-5′	GAAGGTATGAATGGCGTGAG
prsB-3′	AAGCAACTCCATCAGACCGTCGT
prsC-5′	CTATTGGGAACTTATCGC
prsC-3′	GGTCTGTGATCCGCGTGGGACGG
RT-actin-L	TCTTCCAGCCCAGCGTTCT
RT-actin-R	GGGCGGTGATTTCCTTCTG

Table 2. cont.

Primer name	DNA sequence 5′–3′
RT-*AnprsA*-L	ATCTCCTCACAGTTGCTGGGGTTG
RT-*AnprsA*-R	GAAAGGCTCGGCGAATAGGTTGT
RT-*AnprsB*-L	GAACCAGGAAACAAGCGTGACAA
RT-*AnprsB*-R	AAGCAACTCCATCAGACCGTCGT
RT-*AnprsC*-L	TGTGAGCCCAGACGCTGGTGGCG
RT-*AnprsC*-R	GGTCTGTGATCCGCGTGGGACGG
N-*AnprsA*-L	GGAGGGACGAAACGAGTAAC
N-*AnprsA*-R	ACAGCCCATAGATGTAGGACCAG
N-*AnprsB*-L	CGACTGCAATCGCCGATC
N-*AnprsB*-R	TGTGGGAAAACAGGAAGC
N-*AnprsC*-L	TCTCCCGCTCTTTCCATACT
N-*AnprsC*-R	TTGAGCCACCCACTGTTTAT
gpd-L	GAATTCCCTTGTATCTCTACACA
gpd-R	GGAAATAAAGGTTCTTGGATG
G-*AnprsA*-L	CCCCTCATTCTTGAATCGGGAAATAAAGGTTC TTGGATG
G-*AnprsA*-R	TGGTTTTCGTTTGCTAATTTGGCGGGTAAG TCAGATAATAG
G-*AnprsB*-L	CAGTGTCGAGCAAGCGGA GGAAATAAAGGTTC TTGGATG
G-*AnprsB*-R	ACCTTATTATGCCGTCGG TTGGCGGGTAAG TCAGATAATAG
G-*AnprsC*-L	TAGATGCGAGGCGAGCAA GGAAATAAAGGTTC TTGGATG
G-*AnprsC*-R	CATGTCTTACCGCCAACC TTGGCGGGTAAG TCAGATAATAG
pyroA-L	TTGGCGGGTAAGTCAGATAATAG
pyroA-R	CTGACTTGACGCTTTCTCTTGG

C3206, China) according to the manufacturer's instructions [43, 44].

RNA isolation for Northern analysis and real-time PCR

The wild-type TN02A7 strain was grown in liquid medium MMPGRUU at 37 °C for 6 h or 18 h and then transferred into solid MMPGRUU medium for 24 h. We then pulverized the mycelia of those strains to fine powder in the presence of liquid nitrogen. RNA purification and Northern blot analysis were performed as previously described. Briefly, the total RNA was extracted using TRIzol (Roche) following the manufacturer's instructions. We used 100 mg of each mycelia per sample as the starting material for the determination of total RNA and then transferred the sample to a nylon membrane. The blots were probed with ^{32}P-labelled oligonucleotide probes complementary to the mRNA of *AnprsA*, *AnprsB* and *AnprsC*. The primer sequences of the oligonucleotide probes used for the Northern blots are listed in Table 2. The samples from the same cultivation conditions described above were treated with DNase I (TaKaRa), and reverse transcription PCR (RT-PCR) was carried out using the SuperScriptIII first-strand synthesis system (Invitrogen, 18080-051); cDNA was generated using an iScript Select cDNA synthesis kit (Bio-Rad). Real-time PCR was

performed using an ABI one-step fast thermocycler (Applied Biosystems), and the reaction products were detected with SYBR green (TaKaRa). PCR was accomplished by a 10 min denaturation step at 95 °C, followed by 40 cycles of 30 s at 95 °C, 30 s at 60 °C and 30 s at 72 °C. The transcript levels were calculated by the comparative $2^{\triangle CT}$ method and normalized against the expression of the actin gene in *Asp. nidulans*. Primer information is provided in Table 2 [45, 46].

Assay of AnPrs activity

Phosphoribosyl pyrophosphate synthetase activity was assayed following a modified version of as described in previous reference [47]. Briefly, conidial spores were inoculated in derepressing condition medium and then shaken at 220 r.p.m. at 37 °C for 18 h. Then, the spores were transferred to repressing conditions and allowed to cultivate for 6 h. The mycelia were then resuspended in 1 ml of extraction buffer (50 mM KH_2PO_4/K_2HPO_4 at pH 7.5, 10.00 % glycerol, 0.10 % Triton X-100, 5 mM $MgCl_2$, 1 mM EDTA, 1 mM EGTA, 1 mM PMSF and 5 mM DTT) and disrupted by MP Fast-Prep 24 before being clarified by centrifugation (10 000 ***g*** for 15 min at 4 °C). Measurements were performed in microplates by mixing 10 µl of the supernatant of the enzyme extract with 100–200 µl of measuring buffer (KH_2PO_4/K_2HPO_4 at pH 7.5, 5 mM $MgCl_2$, 3.75 mM R5P, 2 mM ATP, 3.75 mM phosphoenolpyruvate, 0.2 mM NADH, 1.5 U myokinase, 3 U pyruvate kinase and 1.5 U lactate dehydrogenase). The oxidation of NADH was measured by monitoring absorption at 340 nm using a Multiskan Spectrum (Thermo Electron, Waltham, MA, USA) at room temperature. The specific activity of AnPrs is expressed as µmol min^{-1} (mg of NADH oxidized)$^{-1}$ using the molar extinction coefficient of 6220 M^{-1} cm^{-1} for NADH. The soluble protein content of the supernatant was determined using a dye binding assay [48].

Constitutive overexpression of *AnprsA*, *AnprsB* and *AnprsC* in the background of the conditional strain *alc(p)-gfp-AnprsB*

A plasmid containing the *gpd*A-*AnprsA*-*pyroA* fragment was created by double joint PCR. The *Asp. nidulans pyroA* gene in plasmid pQa-pyroA was used as a selectable nutritional marker for fungal transformation. The linearized DNA fragment 1 is included in a sequence of approximately 2172 bp of the constitutive overexpression promoter *gpd*A and was amplified with the primers *gpd*-L and *gpd*-R (Table 2). Linearized DNA fragment 2, which included a sequence of approximately 1801 bp of the ORF of the *AnprsA* genes from the genome DNA of TN02A7, was amplified with primers G-*AnprsA*-L and G-*AnprsA*-R (Table 2). Finally, purified linearized DNA fragments 1 and 2 plus the *pyroA* gene were mixed and used in a fusion PCR with primers G-*AnprsA*-p2 and G-*AnprsA*-p5. The final fusion PCR products were purified and loaded into the commercial vector plasmid pEasy-Blunt Zero. Then, those constitutive overexpression plasmids were transformed into *Asp. nidulans* conditional strains *alc(p)-gfp-AnprsB* and cultivated in repressing medium. A diagnostic PCR assay was performed to identify the fusion fragment by primers *gpd*-L and *pyroA*-R. A similar strategy was used to construct the *AnprsB* and *AnprsC* constitutive overexpression strains which were then transformed to *alc(p)-gfp-AnprsB* [49].

RESULTS

Identification and phylogenetic analysis of three PRPP synthetase proteins in *Asp. nidulans*

To search for and identify the Prs homologues in *Asp. nidulans*, the protein sequence of budding yeast ScPrs1p was used as query via protein blast in NCBI. AnPrsA encoded by AN6711.4 and two additional Prs homologues in *Asp. nidulans* were found. One of these was encoded by AN1965.4 and shared 30.60 % protein sequence identity to AnPrsA, here referred to as AnPrsB. In comparison, another homologue protein encoded by AN3169.4 shares 26.90 % protein sequence identity to AnPrsA; we designated this protein as AnPrsC. To further gain insight into the sequence information for the AnPrs family, we compared these three proteins by sequence alignment. Although the length of these three proteins was different, they all shared the two conserved domains that identify them as Prs proteins. One belongs to the N-terminal domain of ribose phosphate pyrophosphokinase (Pribosyltran-N), and the other one is the phosphoribosyl transferase (PRTases type I) domain (Fig. 1a). To further analyse the evolutionary relationship between the AnPrs family and Prs homologues in *S. cerevisiae* in which the functions of Prs have been verified, we created a neighbour-joining tree based on the amino acid sequences of ScPrs1p-5p and AnPrsA-C homologues. The tree-view results indicated that AnPrsA is clustered together with ScPrs1p to form a group, whereas AnPrsB shared the same cluster as ScPrs2p, ScPrs3p and ScPrs4p. Notably, AnPrsC is most likely a putative homologue of ScPrs5p based on the phylogenetic relationship and the amino acid sequence identity (Fig. 1b). Furthermore, as shown in Fig. 1(c), the three Prs proteins in *Asp. nidulans* are conserved in all *Aspergillus* species.

Individual gene knockout experiments show that *AnprsB* and *AnprsC* but not *AnprsA* are auxotrophic genes

To verify the biological function for each of the AnPrs proteins, the knockout strains for *AnprsA*, *AnprsB* and *AnprsC* genes were constructed individually using *AfpyrG* as the nutritional marker. PCR analysis showed that the *AfpyrG* nutritional marker was integrated into the genome at the original *AnprsA*, *AnprsB* and *AnprsC* loci (Fig. S1a, available in the online Supplementary Material). For the deletion strain of *AnprsA*, there was no detectable PCR band, indicating that the *AnprsA* whole-gene deletion mutant had been successfully constructed. Phenotypic analysis suggests that, except for the slightly slow growth rate, the deletion of *AnprsA* had no detectable effect on cellular morphology compared to that of the parental wild-type strain (Fig. 2a). For the *AnprsB* and *AnprsC* deletion strains, even when the ORFs of *AnprsB* and *AnprsC* were replaced with the nutritional marker *AfpyrG*, the

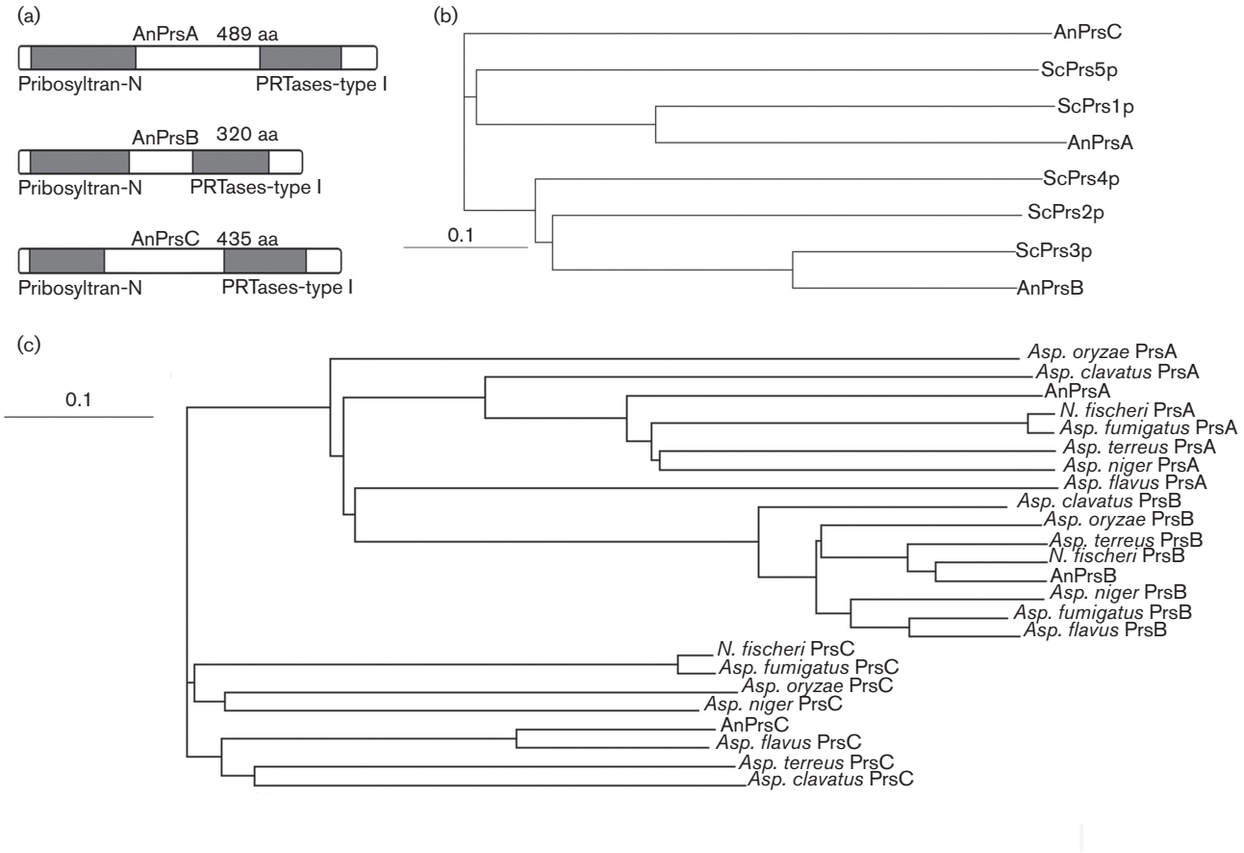

Fig. 1. Bioinformatic and phylogenetic analysis of AnPrs homologues in selected *Aspergillus* species compared to that in *S. cerevisiae.* (a) Schematic diagram of the conserved domain in AnPrs family. Three AnPrs members all contain two conserved protein domains belonging to a Probosyltran-N domain family and PRTases-type I domain family based on a SMART protein search (http://smart.embl-heidelberg.de/). The numbers in the middle of each diagram indicate the varied length of amino acids in these three proteins. (b) The phylogenetic tree was constructed via MEGA 5.2. NCBI accession numbers of PRPP synthetase family in *S. cerevisiae* are ScPrs1p (YKL181W), ScPrs2p (YER099C), ScPrs3p (YHL011C), ScPrs4p (YBL068W) and ScPrs5p (YOL061W) and phylogenetic tree representing the evolutionary relationship between AnPrs family and PRPP synthetase family in *S. cerevisiae.* The tree shows that AnPrsA is close to ScPrs1p; AnPrsB is the potential orthologue to ScPrs2p, ScPrs3p and ScPrs4p; and AnPrsC is the homology to ScPrs5p. The scale bar represents genetic divergence of length 0.1 in units of amino acid substitutions per site.(c) Phylogenetic analysis of Prs homologues in selected *Aspergillus* species. Amino acid sequences were aligned with a CLUSTALW multiple sequence alignment programmes and the phylogenetic tree was constructed shown via MEGA 5.2. Organism sources and NCBI accession numbers are *Aspergillus oryzae* PrsA (AO090005000432), PrsB (AO090003001133) and PrsC (AO090012000798); *Aspergillus clavatus* PrsA (ACLA007390), PrsB (ACLA049960) and PrsC (ACLA041080); *Nassarius fischeri* PrsA (NFIA026920), PrsB (NFIA105300) and PrsC (NFIA063980); *Aspergillus fumigatus* PrsA (Afu7g05670), PrsB (Afu4g10790) and PrsC (Afu3g13380); *Aspergillus terreus* PrsA (ATEG06364), PrsB (ATEG03990) and PrsC (ATEG04065); *Aspergillus niger* PrsA (An07g02210), PrsB (An04g05860) and PrsC (An02g09240); and *Aspergillus flavus* PrsA (AFL2G00420), PrsB (AFL2G01905) and PrsC (AFL2G03660);The scale bar represents genetic divergence of length 0.1 in units of amino acid substitutions per site. Abbreviation: aa, amino acids.

AnprsB and *AnprsC* genes could still be detected, indicating the existence of a possible heterokaryon, as shown in Fig. S1(c, d). To better observe the resultant phenotype, we inoculated the haploid asexual spores from the transformants onto the selective solid media YAG; they were unable to germinate normally or form detectable colonies. However, when replicated on non-selective YUU medium, the spores germinated and formed colonies during the same culture time. According to the standard protocol to detect essential genes as previously described, the deletion of *AnprsB* or *AnprsC* resulted in transformants only capable of surviving as the heterokaryon hyphal form [41]. These heterokaryotic hyphae included two genetically distinct types of nuclei in the same cell. The genotypes of these two types of nuclei are $pyrG^{-}$/(*AnprsB*$^{+}$ *or AnprsC*$^{+}$*)* and $pyrG^{+}$ (Δ*AnprsB or* Δ*AnprsC*). Thus, using the previously described heterokaryon rescue technique, as shown in Fig. 2(b), we identified that both *AnprsB* and *AnprsC* may be essential genes. However, there was another alternative explanation for this observation; Δ*AnprsB* and Δ*AnprsC* may confer auxotrophies that were insufficiently supplemented in

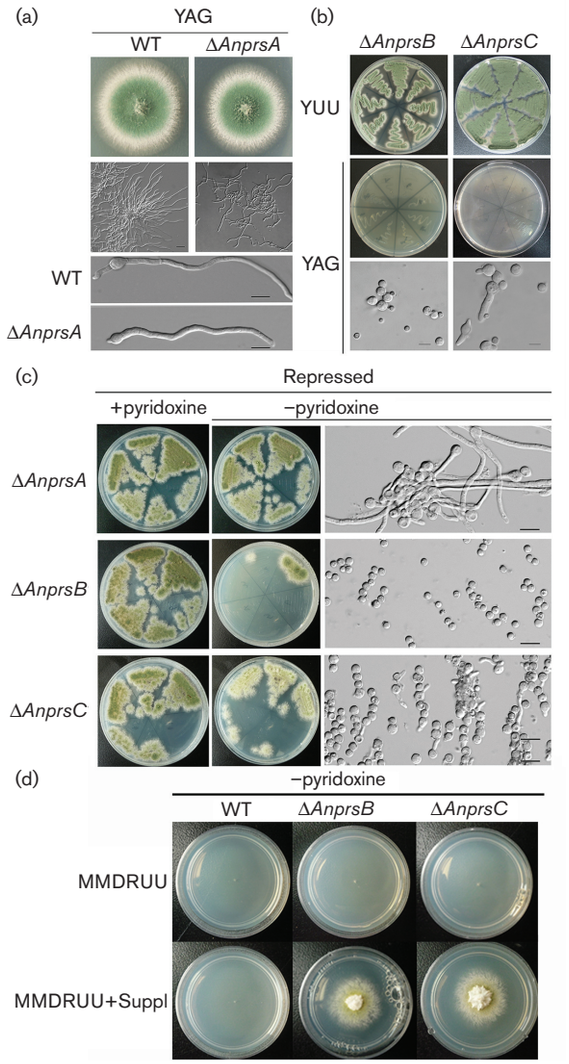

Fig. 2. Phenotypic characterizations of the *AnprsA*, *AnprsB* and *AnprsC* gene deletion mutants. (a) The Δ*AnprsA* strain showed the reduced colony and hyphal growth phenotype compared to the parental wild-type. Upper panel: Colony phenotypic comparison of Δ*AnprsA* strain and wild-type (WJA01) cultured on YAG medium for 2 days, respectively. Middle and lower panels: Hyphal growth comparison of Δ*AnprsA* strain and wild-type cultured in liquid selective medium YAG for 12 h, respectively. Bars, 10 µm. (b) Heterokaryon rescue analysis of Δ*AnprsB* and Δ*AnprsC* strains. Upper and middle panels: Spores of Δ*AnprsB* and Δ*AnprsC* heterokaryons cultured on solid media YUU and YAG for 2 days. Lower panel: Conidia of heterokaryon transformants cultured in liquid medium YAG for 2 days. Bars, 10 µm. (c) Upper panel: Colony phenotypic comparison of Δ*AnprsA* strain selected by *AnpyroA* cultured on MMPDRUU and MMDRUU media for 2.5 days, respectively. Hyphal growth cultured in liquid selective medium MMDRUU for 12 h. Bars, 10 µm. Middle and lower panels: Different concentration of spores of Δ*AnprsB* and Δ*AnprsC* heterokaryon cultured on solid media MMPDRUU and MMDRUU for 2.5 days. Conidia of heterokaryon transformants cultured in liquid medium MMDRUU for 12 h. Bars, 10 µm. (d) The colony morphology of parental wild-type and deletion strains of *AnprsB* and *AnprsC* by *AnpyroA* grown on the selective medium MMDRUU was supplemented with the predicted downstream products or not for 2.5 days.

the selection media, or these genes may be required for function of the *AfpyrG* selectable marker since *Anprs* is the metabolic step immediately upstream of *pyrG* in the metabolic pathway. To get rid of this concern, *AnprsB* and *AnprsC* genes were deleted again using another selectable marker *pyroA*. As a result, for the *AnprsB* and *AnprsC* deletion transformants that the *AnpyroA* nutritional marker had been integrated into the genome at the original *AnprsB* and *AnprsC* loci, the *AnprsB* and *AnprsC* genes could still be detected as shown in Fig. S1(g, h), indicating that the purified *AnprsB* and *AnprsC* deletion strains were not obtained. In comparison, *AnprsA* deletion strain was easily purified. It suggests that the *AnprsB* and *AnprsC* genes could be essential or auxotrophic and it also indicates the existence of a possible heterokaryon in transformants. Further phenotypic examination indicated that conidia from most of the *AnprsB* and *AnprsC* deletion transformants were unable to germinate normally or form detectable colonies in the selective media without pyridoxine, indicating that the *AnprsB* and *AnprsC* genes could be essential or auxotrophic. However, when replicated on non-selective media with pyridoxine, the spores germinated and formed colonies during the same culture time, suggesting that those transformants were heterokaryotic (Fig. 2c). In comparison, some conidia from a few transformants were capable of forming colonies on the selective media but diagnostic PCR verified that these colonies were not gene replacements of *AnprsB* or *AnprsC*. These data collectively demonstrated the *AnprsB* and *AnprsC* genes are essential or deletion of these genes confers auxotrophic requirements.

To further observe the microscopic phenotypes of these two deletion transformants, the haploid asexual spores were cultured in liquid selective medium YAG or MMDRUU. Δ*AnprsB* showed no detectable signs of germination. Most of the spores had not undergone isotropic growth, which resulted in the original state of the conidia being maintained.In comparison, a portion of the Δ*AnprsC* transformant spores were in the original state; however, some spores completed isotropic growth but could not continue to form mature hyphae, which instead formed a small number of short germlings. (Fig. 2b, c). To determine whether the related downstream metabolites catalysed by the Prs enzyme could rescue the growth defect phenotype in the *AnpyroA*-fused Δ*AnprsB* and Δ*AnprsC* heterokaryotic transformants, the predicted downstream products (uracil/uridine, adenine, guanine, histidine, tryptophan and AMP) were supplemented in the selection medium MMDRUU. As shown in Fig. 2(d), when the medium was supplemented with these downstream products, spores from the *AnprsB* or *AnprsC* deletion heterokaryon were able to form colonies in the absence of pyridoxine (Fig. 2c). We then streaked spores to isolate the single colony for which the wild-type *AnprsB* and *AnprsC* genes are absent by diagnose PCR assay, indicating that Δ*AnprsB* and Δ*AnprsC* are purified. These data suggest that *AnprsB* and *AnprsC* are auxotrophs rather than essential genes (Fig. S3a, b). Above results indicate that deletion of *AnprsB* or *AnprsC* confers auxotrophic requirements of PRPP downstream products.

Conditional strains further confirm that *AnprsB* and *AnprsC* are auxotrophic genes

Aforementioned data suggest that *AnprsB* and *AnprsC* are auxotrophic genes; it is difficult to study their cellular function in detail by using the deletion strains. Instead, conditional strains were used. Thus, we constructed conditional strains in which the *AnprsA*, *AnprsB* and *AnprsC* genes were under the control of the derepressible/repressible/inducible *alc*A promotor as regulated by the carbon source: repressed on glucose, derepressed on glycerol and induced on threonine. As illustrated in Fig. S2, the diagnostic PCR results indicated that three conditional strains were constructed as expected for homologous integration. We referred to *alc(p)-gfp-AnprsA* as ZGA01, *alc(p)-gfp-AnprsB* as WFA03 and *alc(p)-gfp-AnprsC* as WFA04. Western blot analysis showed that the molecular size of the GFP fusion protein was consistent with single-copy homologous integration at the *AnprsA*, *AnprsB* and *AnprsC* loci, respectively, in the derepressed medium as shown in Fig. 3(b). In contrast, under the repressed condition, these bands vanished completely, thus indicating the functionality and specificity of the alcohol-inducible *alcA* promoter in these three conditional strains. GFP-AnPrsA, GFP-AnPrsB and GFP-AnPrsC all exhibited the cytosol localization pattern but showed exclusion in the nuclear region (Fig. 3a). When these three conditional strains were inoculated on the derepressing medium (i.e. with glycerol as the sole carbon source) for 2.5 days at 37 °C, the colony size of these conditional strains was almost similar to that of the parental wild-type strain, indicating that the resulting GFP-AnPrsA, GFP-AnPrsB and GFP-AnPrsC fusions were functional in the derepressing media. In comparison, when they were grown on the repressing medium that contained glucose, AnPrsA conditional strain ZGA01 displayed an almost normal colony phenotype except with a slightly small size. As expected, neither conditional strain [AnPrsB (WFA03) or AnPrsC

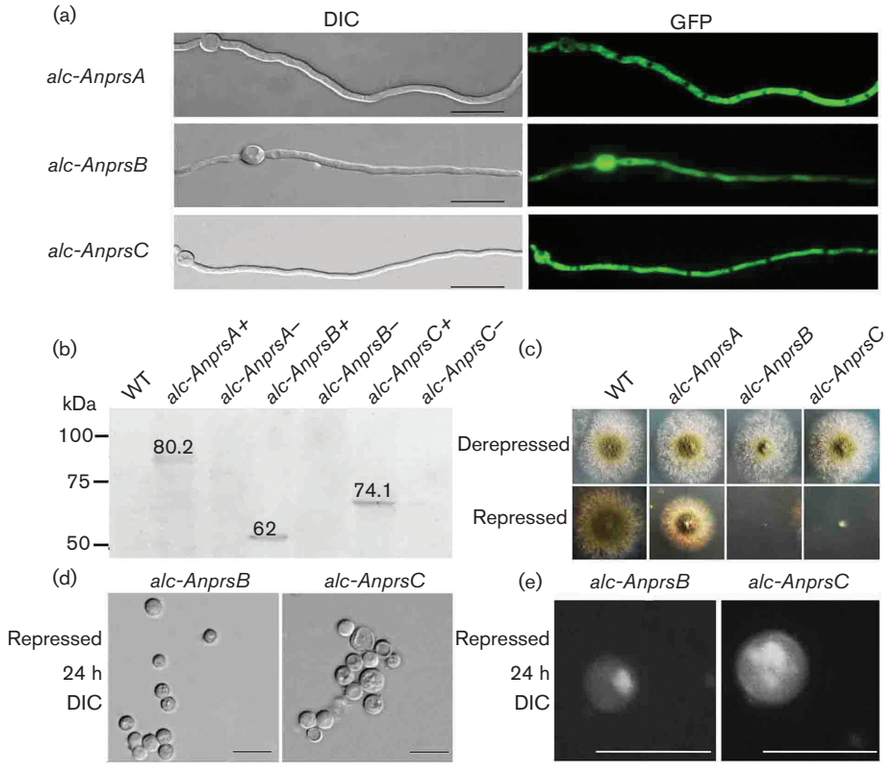

Fig. 3. Localization and phenotypic characterization of GFP-AnPrsA, GFP-AnPrsB and GFP-AnPrsC in the *alcA(p)-gfp-AnprsA*, *alcA(p)-gfp-AnprsB* and *alcA(p)-gfp-AnprsC* strains. (a) The localization pattern of AnPrsA, AnPrsB and AnPrsC under the derepressing medium MMPGRUU for 16 h; GFP-AnPrsA, GFP-AnPrsB and GFP-AnPrsC all exhibited cytosolic localization patterns but exclude the nuclear region. Bars, 10 µm. (b) Western blotting indicates that the GFP-AnPrsA, GFP-AnPrsB and GFP-AnPrsC fusion proteins were detected by the anti-GFP antibody at the predicted sizes of about 80.2, 62 and 74.1 kDa, respectively. + and – indicate depressing and repressing. (c) Colony phenotypic comparison of the parental wild-type (WJA01), *alcA(p)-gfp-AnprsA* (ZGA01), *alcA(p)-gfp-AnprsB* (WFA03) and *alcA(p)-gfp-AnprsC* (WFA04) conditional strains on the solid derepressing medium (MMPGRUU) and repressing medium (MMPDRUU) for 2.5 days, respectively. (d) Conidiospore germination phenotypic comparisons of *alcA(p)-gfp-AnprsB* and *alcA(p)-gfp-AnprsC* cultured in the repressing liquid medium MMPDRUU for 24 h respectively. Bars, 10 µm. (e) Nuclei staining phenotypic comparison of germlings in *alcA(p)-gfp-AnprsB* and *alcA(p)-gfp-AnprsC* cultured in the repressing liquid medium MMPDRUU for 24 h, respectively. The nuclei were stained with DAPI. Bars, 5 µm.

(WFA04)] could form visible colonies, thus suggesting that *AnprsB* and *AnprsC* are auxotrophic genes. This finding also suggests that, on the repressing medium, three conditional strains displayed a consistent phenotype with the deletion strains, indicating that the *alc*A promoter was able to be shut off efficiently under the repressed condition (Fig. 3c). To analyse the microscopic phenotypes during the loss of *AnprsB* or *AnprsC* individual function, the conidia of WFA03 and WFA04 were inoculated in the liquid repressing medium for 24 h at 37 °C. WFA03 did not show any signs of isotropic growth, including only one DAPI-stained nucleus inside the cell, indicating that mitosis was arrested in the absence of *AnprsB*. In comparison, in WFA04, there were approximately 4–6 nuclei inside the enlarged spore, which was almost twice the size of the normal parental wild-type conidium, thus indicating that the loss of function of *AnprsC* was unable to stop mitosis immediately but resulted in an extended spore isotropic period (Fig. 3d, e).

Since we used *pyrG* as a selection marker while *Anprs* is upstream of *pyrG* in the pyrimidine biosynthesis pathway, to determine whether the *AnprsB* and *AnprsC* genes confer an auxotrophic requirement for growth rather than are essential, we inoculated these conditional strains on the repressing medium MMPDR with or without UU addition, respectively. As shown in Fig. 4, under the repressing condition, the AnPrsA conditional strain formed normal colonies similar to its parental wild-type strain. However, no detectable colonies were formed in conditional strain WFA03 or WFA04 for repressed *AnprsB* or *AnprsC*, no matter whether UU (uridine + uracil) was added or not on the repression medium MMPDR. This result indicates that the phenotype of growth inhibition in *AnprsB* and *AnprsC* conditional strains was due to turn off the gene expression of *AnprsB* and *AnprsC* but not due to the absence of the function of the *pyrG* selectable marker. Furthermore, to detect if the related downstream metabolites catalysed by the Prs enzyme could rescue the growth defect in *AnprsB* and *AnprsC* mutants, the predicted downstream products histidine, tryptophan, pyrimidine and AMP were added to the medium MMPDRUU. As expected, the auxotrophic phenotype of *AnprsB and AnprsC* could be significantly rescued to some extent. It further indicates that *AnprsB* and *AnprsC* are involved in the *de novo* and salvage purine and pyrimidine nucleotide pathways and in the biosynthesis of nucleotide coenzymes, histidine and tryptophan production. Phenotypic analysis demonstrates that the absence of the *AnprsB* or *AnprsC* gene product confers auxotrophy for uracil/uridine, adenine, guanine, histidine, tryptophan and/or AMP. The lack of repair with uracil/uridine alone likely indicates that at least one (or possibly all) of adenine, guanine, histidine, tryptophan or AMP is also required, i.e. repressing *AnprsB* or *AnprsC* expression results in auxotrophy for one or more of uracil/uridine, adenine, guanine, histidine, tryptophan or AMP. Above results further confirm that deletion of *AnprsB* or *AnprsC* gives rise to auxotrophy and are auxotrophic genes.

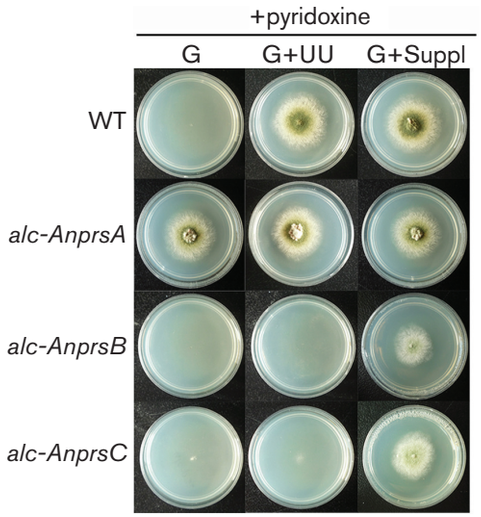

Fig. 4. Conditional strains further confirm that *AnprsB* and *AnprsC* are auxotrophic genes. The colony morphology of three AnPrs conditional strains and its parental wild-type grown on the repressed medium MMPDR (the glucose-containing medium: G), MMPDRUU (G+UU) or MMPDR supplemented by all of the downstream products of phosphoribosyl pyrophosphate synthetase (G+Suppl) at 37 °C for 2.5 days. Abbreviations: G, glucose; UU, uracil/uridine, Suppl, adenine + guanine + histidine + tryptophan + AMP.

AnprsB and *AnprsC* but not *AnprsA* are required during hyphal elongation

According to previous reports, when conidia were cultured in liquid medium for 7 h, most conidia germinated to form germlings. The 7 h liquid culture time was referred to as the germination time point and the 18 h liquid culture time was a vigorous hyphal growth time point. When the 18 h liquid cultures were transferred to the solid culture plate for 24 h, this time point was referred to as the sporulation period [50–52]. To further verify the time course of biological function for the *Anprs* family, we turned off three *Anprs* genes individually during the aforementioned different development stages. As shown in Fig. 5(a), when expression of *AnprsA* was halted during germination or the vigorous hyphal growth time point, germlings could be formed with a continually robust hyphal growth that was normal in the conditional strain compared to its parental wild-type strain. In comparison, the hyphal growth in repressed media from transferred germlings in conditional medium expressing *AnprsB* or *AnprsC* appeared to be almost halted. Through quantitative testing, the extended length of hyphae was a reduction of approximately 62.28 ±1.00 % lower than those of the parental wild-type strain when *AnprsC* was turned off in the MMPDRUU medium. Moreover, under the same culture condition as those described above, the inhibited expression of *AnprsB* resulted in more severe hyphal extension defects than did *AnprsC*, with a hyphal length that was significantly decreased by 80.00±2.00 % compared with the length in

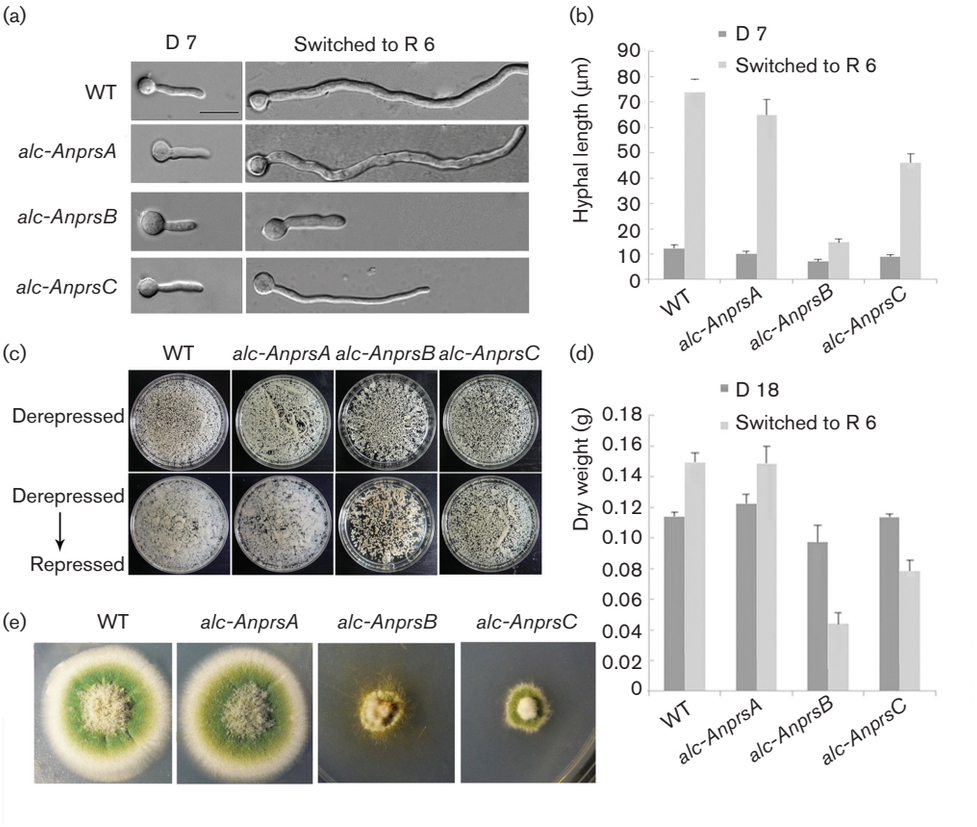

Fig. 5. AnPrsB and AnPrsC but not AnPrsA are required for hyphal elongation. (a) Germling phenotypic comparison of parental wild-type (TN02A7), *alcA(p)-gfp-AnprsA*, *alcA(p)-gfp-AnprsB* and *alcA(p)-gfp-AnprsC* cultured in the liquid derepressing medium MMPGRUU for 7 h (D 7) and then switched to repressing liquid media MMPDRUU for 6 h (R 6), respectively. Bars, 10 μm. (b) The quantitative data of hyphal length for (a). Error bars represent the SD of three replicates (Duncan's multiple range tests, $P<0.05$). (c) A cultured equal number of conidia of wild-type and conditional strains in 100 ml liquid derepressing medium MMPGRUU at 220 r.p.m. for 18 h (D 18). We then transferred the derepressed mycelia into 100 ml liquid repressing medium MMPDRUU at 220 r.p.m. for 6 h (R 6). The reference strains were cultured in derepressing medium for 6 h, and we then poured the mycelium pellet onto a plate to observe the phenotype. (d) Quantitative data for the dry weight of the conditional and reference strains at (c). Error bars represent SD values from three replicates (Duncan's multiple range tests, $P<0.05$). (e) Colonies of the parental wild-type strain TN02A7 and the conditional strains *alcA(p)-gfp-AnprsA*, *alcA(p)-gfp-AnprsB* and *alcA(p)-gfp-AnprsC* in the liquid derepressing medium MMPGRUU for 18 h and then transferred into the repressing solid medium MMPDRUU for 24 h to form colonies.

the parental control strains (Fig. 5b). Similarly, we tested the inhibition of the growth of mycelia in liquid medium when the expression of the *Anprs* gene family was inhibited. As shown in Fig. 5(c), repression of *AnprsB* and *AnprsC* remarkably inhibited the hyphal elongation during the hyphal growth stage. Through quantitative testing, the dry weight of the *alc(p)-gfp-AnprsB* and *alc(p)-gfp-AnprsC* strains was approximately 3.40- and 1.88-fold lower, respectively, than those of the parental wild-type strain on MMPDRUU (Fig. 5d). To detect the function of the *AnprsA*, *AnprsB* and *AnprsC* genes during the sporulation period, we switched the relative conditional strains from the derepressed medium to the repressed medium during the sporulation stage. As shown in Fig. 5(e), unlike at the hyphal growth time point, inhibiting the expression of *AnprsA* or *AnprsB* or *AnprsC* during the sporulation stage was unable to affect conidiation, suggesting that *AnprsB* and *AnprsC* are both required for hyphal growth but all members of *AnprsA–C* are not required for sporulation.

The mRNA levels for the *Anprs* family and the contribution to the total Prs enzyme activity

Genomic information analyses indicated that all of the *AnprsA*, *AnprsB* and *AnprsC* genes encode homologues of phosphoribosyl pyrophosphate synthetase, which implies that *AnprsA*, *AnprsB* and *AnprsC* may cause similar defective phenotypes. However, as mentioned above, *AnprsB* and *AnprsC* are auxotrophic genes, but *AnprsA* is not, indicating that the functions of those three genes are markedly different. To better understand the function of the three AnPrs

genes, Northern blotting and real-time PCR analysis were carried out to visualize the mRNA abundance levels of these three *Anprs* genes in various developmental stages. 28S and 18S RNA was the loading control for Northern blotting and actin was used as an internal reference for real-time PCR analysis, as shown in Fig. 6(a, b). As a result, at the germination time point (G 7), the *AnprsA*, *AnprsB* and *AnprsC* transcripts were only 10.00 %, 10.00 % and 8.00 % of the level of the relative expression of actin, respectively. In comparison, at the vigorous hyphal growth time point (V 18), the mRNA levels of *AnprsA*, *AnprsB* and *AnprsC* reached nearly 96.00, 27.00, and 68.00 % of the actin levels, respectively. However, the transcription of all three genes declined to the lowest level during the sporulation phase such that only 5.00 % of the *AnprsB* and *AnprsC* transcripts to the level of actin were left, compared to 12.00 % of the *AnprsA* in the same period. Therefore, these data indicate that the *AnprsA*, *AnprsB* and *AnprsC* genes have their own expression profiles at the different development stages.

These phenomena led us to consider that the contribution of different AnPrs proteins may be unequal to the contribution of Prs enzyme activity. To test this hypothesis, biochemical assays for testing PRPP synthetase activity were performed according to the standard protocols described in the experimental procedures. Three *Anprs* conditionals and the corresponding reference strains were cultured on the repressed medium to turn off the expression during the vegetative stage. Consequently, repression of *AnprsB* expression in WFA03 markedly blocked the PRPP production, leaving only 49.00 ±8.00 % of the Prs enzyme activity compared to the parental wild-type. In comparison, the elimination of *AnprsC* expression left nearly 73.00±2.00 % of the Prs enzyme activity compared that in parental wild-type strain. However, when the *AnprsA* conditional strain ZGA01 was cultured under the same repressing condition, it was able to keep almost 86.00 ±1.00 % of the Prs enzyme activity (Fig. 6c). Taken together, these results suggest that PRPP synthetase activity was predominately dependent on the transcription level of *AnprsB*, followed by *AnprsC* and then *AnprsA*.

Functional complementation test in the AnPrs family

According to the above results, *AnprsB* and *AnprsC* probably have major roles in the AnPrs family for their contribution to Prs enzyme activity. Therefore, the deletion of *AnprsB* or *AnprsC* causes the growth inhibition, indicating that normally expressed AnPrsA, AnPrsC or AnPrsA, AnPrsB could not rescue the deleted function of *AnprsB* or *AnprsC*, respectively. To gain further insight into whether *AnprsB* is irreplaceable, we carried out the functional complementation test to examine the constitutive overexpression of *AnprsA* and *AnprsC* in the background of the repressed *AnprsB* strain. A full-length ORF sequence of *AnprsA* or *AnprsB* or *AnprsC* under the constitutive control of the *gpd*A promoter was separately transformed

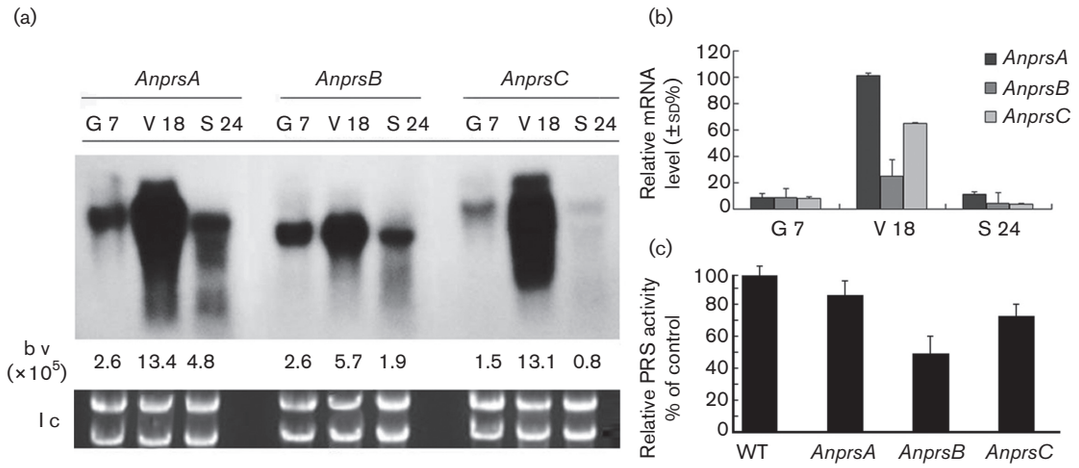

Fig. 6. The mRNA levels for the *Anprs* family and the contribution to the total Prs enzyme activity. (a) Expression levels of *AnprsA*, *AnprsB* and *AnprsC* mRNA were shown by Northern blot analysis with RNA extracted from the wild-type strain throughout three developments stages. The capital letters, G 7, V 18 and S 24, indicate the germination time point (G 7), vigorous hyphal growth time point (V 18) and sporulation period (S 24), respectively. Equal loading of RNA samples was evaluated by 28S and 18S RNA bands(l c :loading control). Numbers below the blots denoted the relative density of each band normalized as calculated using ImageJ (b v : band volume). (b) The relative mRNA levels of *AnprsA*, *AnprsB* and *AnprsC*, respectively, using a real-time RT-PCR assay in a wild-type strain cultured in liquid MMPGRUU medium at 220 r.p.m. for three developmental stages. The measured quantity of mRNA in each of the treated samples was normalized using C_T values obtained for the internal reference actin (AN3696.4) (c) The fold changes of relative AnPrs enzyme activities of *alc(p)-gfp-AnprsA* (ZGA01), *alc(p)-gfp-AnprsB* (WFA03) and *alc(p)-gfp-AnprsC* (WFA04) after being switched to the repressing liquid medium for 6 h during the vegetative growth stage (V 18) compared to the parental wild-type. The measurements of AnPrs enzyme activity in the three mutant strains were normalized to a percentage compared to wild-type strain TN02A7. Data were the means ± SD of three sets of experiments.

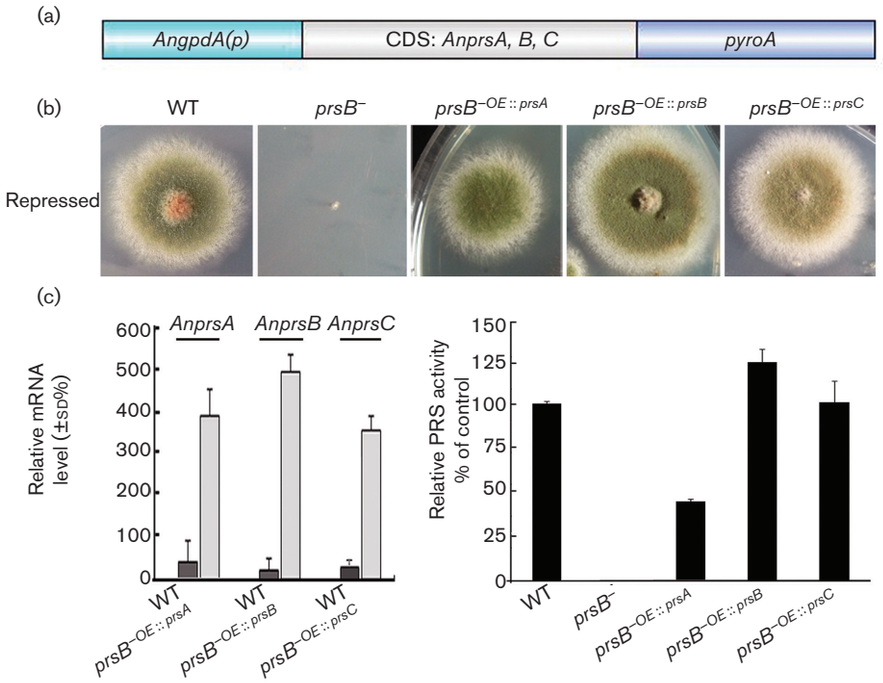

Fig. 7. Functional complementation test in the *alc(p)-gfp-AnprsB* strain under the repressed condition. (a) Illustration of the constitutive overexpression (OE) of the *Anprs* family constructs. The *Asp. nidulans gpd* promoter '*AngpdA(p)*' was used to express *AnprsA*, *AnprsB* and *AnprsC*, respectively. 'CDS' indicates a coding sequence of *AnprsA*, *AnprsB* and *AnprsC* and '*pyroA*' indicates the nutrition marker, respectively. (b) The colony morphology of *AnprsA*, *AnprsB* and *AnprsC* genes overexpressed under the control of '*Angpd(p)*' in the *alc(p)-gfp-AnprsB* strain under the repressed condition. An equal number of conidia (2×10^4) were inoculated in each plate and cultured at 37 °C for 2.5 days. (c) RT-PCR analysis indicated the mRNA level of *AnprsA* or *AnprsB* or *AnprsC* in these OE strains. All mRNA values were normalized to the actin gene. (d) The relative AnPrs enzyme activities of wild-type (TN02A7), *alc(p)-gfp-AnprsB*$^{-}$ (WFA03 in the repressed medium), *alc(p)-gfp-AnprsB*$^{-OE::AnprsA}$ (WFA05), *alc(p)-gfp-AnprsB*$^{-OE::AnprsB}$ (WFA06) and *alc(p)-gfp-AnprsB*$^{-OE::AnprsC}$ (WFA07). Mycelia were grown in liquid YUU medium at 220 r.p.m. and cultured for 2.5 days. Data were normalized to a percentage compared to wild-type strain TN02A7.

into the *alc(p)-gfp-AnprsB* strain on the repressed medium (Fig. 7a, b), resulting in three constitutive overexpression [OE means *gpdA(p)*::*Anprs*] strains that we named WFA05 [*alc(p)-gfp-AnprsB*$^{-OE::prsA}$], WFA06 [*alc(p)-gfp-AnprsB*$^{-OE::prsB}$] and WFA07 [*alc(p)-gfp-AnprsB*$^{-OE::prsC}$]. As shown in Fig. S3 (c), the diagnostic PCR results indicated that three constitutive overexpression strains were constructed successfully. To further ensure that the expression levels of *AnprsA*, *AnprsB* and *AnprsC* in these OE strains were truly overexpressed, quantitative RT-PCR analysis was determined as shown in Fig. 7(c). As expected, the mRNA level of *AnprsA*, *AnprsB* or *AnprsC* in these OE strains was approximately 11.25-, 50.97- or 13.94-fold higher than that in the parental wild-type strain, respectively. As shown in Fig. 7(b), colonies overexpressing *AnprsB* as a gene complementary test showed a similar colony phenotype to the parental strain in regard to colony size and conidiation, indicating that this system, under the control of the *gpd*A promoter, is functional for AnPrsB. Notably, the other OE strains were also able to restore significantly defective hyphal growth to the normal level in the *alc(p)-gfp-AnprsB* conditional strain under the repressed condition. The constitutive overexpression of *AnprsA* could partly rescue the *alc(p)-gfp-AnprsB* defects in the repressed condition with a slightly smaller colony size than the wild-type. In contrast, the constitutive overexpression of *AnprsC* could restore hyphal growth to the wild-type level with a similar colony size to that in the parental strain. However, OE::*AnprsC* was unable to completely rescue the conidiation defect in the repressed *AnprsB* background strain. To further determine whether the above colony rescue phenomena were related to the increased Prs enzyme activity induced by the constitutive overexpression of the *AnprsA* or *AnprsC* gene, we measured Prs enzyme activity. As shown in Fig. 7(d), the total PRPP synthetase activity of OE::*prsB* and *OE*::*prsC* reached almost 126.00 ±1.00 % and 97.00±1.00 %, respectively. However, the *alc(p)-gfp-AnprsB*$^{-OE::prsA}$ strain reached only 45.11±2.00 % of the total PRPP synthetase activity compared to its parental wild-type strain. These data demonstrate that although *AnprsB* is an auxotrophic gene, it is not uniquely irreplaceable because the constitutive overexpression of the non-auxotrophic gene *AnprsA* or the auxotrophic gene *AnprsC* can significantly rescue the growth defect in the *alc(p)-gfp-AnprsB* conditional mutant under the repressed condition.

DISCUSSION

Phosphoribosyl pyrophosphate (PRPP) is an important central compound for cellular metabolism. The formation of PRPP is catalysed by the enzyme PRPP synthetase, which is encoded by Prs genes. Prs genes exist in a variety of organisms to provide unique functions. As indicated by using comparative genomic analyses of *S. cerevisiae PRS1* via BLAST search, we identified three homologous genes *AnprsA*, *AnprsB* and *AnprsC* that encode PRPP synthetases in *Asp. nidulans*. The genome-scale homologue survey revealed that *Anprs* genes are ubiquitous and conserved among selective *Aspergillus* species, such as *Asp. fumigatus*, *Aspergillus niger* and *Asp. oryzae*. Based on the full-length alignment, AnPrsA in *Asp. nidulans* is most closely related to its counterpart in *Asp. fumigatus*, with 92.45 % identity, and is least homologous with its counterpart from *Aspergillus terreus*, with 90.67 % identity (Fig. S4). Comparatively, AnPrsC exhibited the highest identity with *Aspergillus flavus* (95.41 %) and the lowest identity (94.13 %) with *Aspergillus clavatus* (Fig. S5). Most notably, AnPrsB is the most conserved member among Prs members in the selected species in this study, with identities ranging from 98.75 to 99.06 %, as shown in Fig. S6. Moreover, according to the neighbour-joining evolutionary tree analysis, AnPrsA is a putative homologue of yeast ScPrs1p (identity 70.35 %), whereas AnPrsC is most likely a homologue of yeast ScPrs5p (identity 69.88 %). This reduction in identity highlights the existence of non-homologous regions in ScPrs1p and SPrs5p [20]. Most interestingly, AnPrsB is closely related to that of ScPrs2p, ScPrs3p and ScPrs4p in yeast, with identities of 89.10 %, 88.75 and 80.74 %, respectively, suggesting that AnPrsB is likely to be an orthologue of ScPrs2p, ScPrs3p and ScPrs4p (Fig. S7). Previous studies have indicated that, in *H. sapiens*, the missense mutation of HsPRS1 (PRPS1) might be related to many syndromes, indicating that the function of PRPS1 plays an important role in these physiological processes [10–12, 14–16]. As shown in Fig. S8, we found that the AnPrsB protein shares 67.00 % identity with the human disease related protein HsPRS1 (PRPS1) but not HsPRS2 (PRPS2) or HsPRS3 (PRPS1L1). Most interestingly, all sites in PRPS1 with mutations related to human diseases are conserved in AnPrsB (Fig. S8). Therefore, this information suggests that studies on the function of PrsB homologues in a model organism such as *Asp. nidulans* could provide valuable clinical indications and hints for mammalian partners related to genetics and biochemistry.

It has been reported that no single *ScPRS* gene is essential in *S. cerevisiae* but that combined deletions of double (such as *ScPRS1* and *ScPRS5* or *ScPRS3* and *ScPRS5*) or triple member deletions (such as *ScPRS1*, *ScPRS2* and *ScPRS4*) in five *ScPRS* polypeptides could cause a lethal phenotype [53]. This suggests that the five *ScPRS* genes might combine into certain multimeric complexes that are required for PRPP synthetase function. Interestingly, in this study, we found that *AnprsA* is a non-auxotrophic gene but that *AnprsB* and *AnprsC* are auxotrophic genes, i.e. the deletion of either *AnprsB* or *AnprsC* causes an auxotrophic phenotype, and by using conditional strains, we further found that repressing *AnprsB* or *AnprsC* expression results in auxotrophy for more of uracil/uridine, adenine, guanine, histidine, tryptophan or AMP. This phenomenon raises a question of whether the abundant expression of the *AnprsB* and *AnprsC* genes but not *AnprsA* is required during all development stages. However, as shown in Fig. 6(a), our findings indicate that *AnprsA* has an even higher relative expression level than that of *AnprsB* and *AnprsC* at the vigorous hyphal growth time point (V 18). It is possible that the individual function of AnPrsA is unable to support the activity of PRPP synthetase. Instead, the other two *Anprs* genes provide the major PRPP synthetase activity. In addition, our Northern blotting data suggest that the *AnprsA*, *AnprsB* and *AnprsC* genes have their own expression profiles at different developmental stages, indicating that they may cooperate with each other for PRPP synthetase activity. Previous studies have indicated that *Ash. gossypii*, a filamentous hemiascomycete, possesses four nonessential *Agprs* genes (*Aer083cp*, *Agl080cp*, *Agr371cp* and *Adr314cp*) and that these four genes form two homologous heterodimers, AGR371C (Agr371cp-Adr314cp) and AGL080C (Aer083cp-Agl080cp). Compared to AGR371C, AGL080C makes a major contribution to total Prs activity; the double deletion of *Aer083cp* and *Agl080cp* resulted in a large impairment in PRPP synthetase activity accompanied by growth alteration. These data suggest that different Prs members may contribute unequally to PRPP synthetase activity supported by studies of *S. cerevisiae* PRS gene and their products [54]. In comparison, our data demonstrate that PRPP synthetase activity is predominantly dependent on the transcription level of *AnprsB*, followed by *AnprsC* and then *AnprsA* (Fig. 6b, c). Therefore, loss of *AnprsB* or *AnprsC* is unable to allow the PRPP synthetase activity to reach the minimal level required for the growth in the filamentous fungus *Asp. nidulans*. There are two potential explanations for this phenomenon. First, the loss of *AnprsB* or *AnprsC* but not of *AnprsA* function could remarkably decrease the entire Prs enzyme activity in conditional strains, further indicating that AnPrsB and AnPrsC have major roles compared to AnPrsA (Fig. 6c). Second, in addition to being major contributors to the total PRPP synthetase activity, *AnprsB* or *AnprsC* may have multiple auxotrophic roles during morphogenesis. For example, some studies have reported that the constitutive overexpression of *prs* genes could significantly enhance the production of riboflavin in *Ash. gossypii*, indicating that Prs proteins may have other functions required for growth and metabolism aside from the function of total PRPP synthetase activity. In contrast, our data indicate that *AnprsB* is not irreplaceable, even though it is an important auxotrophic gene. Most notably, our results found that the constitutive overexpression (OE) of the *AnprsA* or *AnprsC* gene could rescue the defect of absent *AnprsB* in the conditional strain under the repressed condition. To further determine why overexpressing the other two Prs members could rescue the auxotrophic gene function of *AnprsB*, we detected the total AnPrs enzyme activity in these OE strains. As a result, OE

strains of *AnprsA* and *AnprsC* showed an almost similar level to that of the parental wild-type strain in terms of the total PRPP synthetase activity (Fig. 7). These findings clearly show that the auxotrophic function of *AnprsB* and *AnprsC* is not specific for these genes but is mainly due to the contribution of Prs proteins to PRPP synthetase activity.

Funding information
This work was financially supported by the National Natural Science Foundation of China (NSFC31370112), the Priority Academic Program Development of Jiangsu Higher Education Institutions and the Research to L. Lu and the Special Fund for the Doctoral Program of High Education of China to P. Jiang (no.1812000002152); the plasmid pFNO3 including GFP gene was purchased from Fungal Genetics Stock Center (www.fgsc.net). *Asp. nidulans* strain TN02A7 (AJM68) was a gift of Christopher J. Staiger (Purdue University, West Lafayette).

Conflicts of interest
The authors declare that there are no conflicts of interest.

References

1. Khorana HG, Fernandes JF, Kornberg A. Pyrophosphorylation of ribose 5-phosphate in the enzymatic synthesis of 5-phosphorylribose 1-pyrophosphate. *J Biol Chem* 1958;230:941–948.
2. Hove-Jensen B. Mutation in the phosphoribosylpyrophosphate synthetase gene (*prs*) that results in simultaneous requirements for purine and pyrimidine nucleosides, nicotinamide nucleotide, histidine, and tryptophan in *Escherichia coli*. *J Bacteriol* 1988;170: 1148–1152.
3. Krath BN, Eriksen TA, Poulsen TS, Hove-Jensen B. Cloning and sequencing of cDNAs specifying a novel class of phosphoribosyl diphosphate synthase in *Arabidopsis thaliana*. *Biochim Biophys Acta* 1999;1430:403–408.
4. Jiménez A, Santos MA, Revuelta JL. Phosphoribosyl pyrophosphate synthetase activity affects growth and riboflavin production in *Ashbya gossypii*. *BMC Biotechnol* 2008;8:67.
5. Fang H, Xie X, Xu Q, Zhang C, Chen N. Enhancement of cytidine production by coexpression of *gnd*, *zwf*, and *prs* genes in recombinant *Escherichia coli* CYT15. *Biotechnol Lett* 2013;35:245–251.
6. Breda A, Martinelli LK, Bizarro CV, Rosado LA, Borges CB *et al.* Wild-type phosphoribosylpyrophosphate synthase (PRS) from *Mycobacterium tuberculosis*: a bacterial class II PRS? *PLoS One* 2012;7:e39245.
7. Hove-Jensen B. Phosphoribosylpyrophosphate (PRPP)-less mutants of *Escherichia coli*. *Mol Microbiol* 1989;3:1487–1492.
8. Shi S, Chen T, Zhang Z, Chen X, Zhao X. Transcriptome analysis guided metabolic engineering of *Bacillus subtilis* for riboflavin production. *Metab Eng* 2009;11:243–252.
9. Becker MA, Taylor W, Smith PR, Ahmed M. Overexpression of the normal phosphoribosylpyrophosphate synthetase 1 isoform underlies catalytic superactivity of human phosphoribosylpyrophosphate synthetase. *J Biol Chem* 1996;271:19894–19899.
10. de Brouwer AP, van Bokhoven H, Nabuurs SB, Arts WF, Christodoulou J *et al.* PRPS1 mutations: four distinct syndromes and potential treatment. *Am J Hum Genet* 2010;86:506–518.
11. Kim HJ, Sohn KM, Shy ME, Krajewski KM, Hwang M *et al.* Mutations in PRPS1, which encodes the phosphoribosyl pyrophosphate synthetase enzyme critical for nucleotide biosynthesis, cause hereditary peripheral neuropathy with hearing loss and optic neuropathy (CMTX5). *Am J Hum Genet* 2007;81:552–558.
12. Roessler BJ, Nosal JM, Smith PR, Heidler SA, Palella TD *et al.* Human X-linked phosphoribosylpyrophosphate synthetase superactivity is associated with distinct point mutations in the PRPS1 gene. *J Biol Chem* 1993;268:26476–26481.
13. Yen RC, Adams WB, Lazar C, Becker MA. Evidence for X-linkage of human phosphoribosylpyrophosphate synthetase. *Proc Natl Acad Sci USA* 1978;75:482–485.
14. Li S, Lu Y, Peng B, Ding J. Crystal structure of human phosphoribosylpyrophosphate synthetase 1 reveals a novel allosteric site. *Biochem J* 2007;401:39–47.
15. Liu X, Han D, Li J, Han B, Ouyang X *et al.* Loss-of-function mutations in the PRPS1 gene cause a type of nonsyndromic X-linked sensorineural deafness, DFN2. *Am J Hum Genet* 2010;86:65–71.
16. Mittal R, Patel K, Mittal J, Chan B, Yan D *et al.* Association of PRPS1 mutations with disease phenotypes. *Dis Markers* 2015; 2015:1–7.
17. Alderwick LJ, Lloyd GS, Ghadbane H, May JW, Bhatt A *et al.* The C-terminal domain of the Arabinosyltransferase *Mycobacterium tuberculosis* EmbC is a lectin-like carbohydrate binding module. *PLoS Pathog* 2011;7:e1001299.
18. Lucarelli AP, Buroni S, Pasca MR, Rizzi M, Cavagnino A *et al.* *Mycobacterium tuberculosis* phosphoribosylpyrophosphate synthetase: biochemical features of a crucial enzyme for mycobacterial cell wall biosynthesis. *PLoS One* 2010;5:e15494.
19. Krath BN, Hove-Jensen B. Organellar and cytosolic localization of four phosphoribosyl diphosphate synthase isozymes in *Spinach*. *Plant Physiol* 1999;119:497–506.
20. Ugbogu EA, Wippler S, Euston M, Kouwenhoven EN, de Brouwer AP *et al.* The contribution of the nonhomologous region of Prs1 to the maintenance of cell wall integrity and cell viability. *FEMS Yeast Res* 2013;13:291–301.
21. Mateos L, Jiménez A, Revuelta JL, Santos MA. Purine biosynthesis, riboflavin production, and trophic-phase span are controlled by a Myb-related transcription factor in the fungus *Ashbya gossypii*. *Appl Environ Microbiol* 2006;72:5052–5060.
22. Carter AT, Beiche F, Hove-Jensen B, Narbad A, Barker PJ *et al.* PRS1 is a key member of the gene family encoding phosphoribosylpyrophosphate synthetase in *Saccharomyces cerevisiae*. *Mol Gen Genet* 1997;254:148–156.
23. Hernando Y, Parr A, Schweizer M. PRS5, the fifth member of the phosphoribosyl pyrophosphate synthetase gene family in *Saccharomyces cerevisiae*, is essential for cell viability in the absence of either PRS1 or PRS3. *J Bacteriol* 1998;180:6404–6407.
24. Hove-Jensen B. Heterooligomeric phosphoribosyl diphosphate synthase of *Saccharomyces cerevisiae:* combinatorial expression of the five *PRS* genes in *Escherichia coli*. *J Biol Chem* 2004;279: 40345–40350.
25. Kleineidam A, Vavassori S, Wang K, Schweizer LM, Griac P *et al.* Valproic acid- and lithium-sensitivity in *prs* mutants of *Saccharomyces cerevisiae*. *Biochem Soc Trans* 2009;37:1115–1120.
26. Schneiter R, Carter AT, Hernando Y, Zellnig G, Schweizer LM *et al.* The importance of the five phosphoribosyl-pyrophosphate synthetase (Prs) gene products of *Saccharomyces cerevisiae* in the maintenance of cell integrity and the subcellular localization of Prs1p. *Microbiology* 2000;146:3269–3278.
27. Vavassori S, Wang K, Schweizer LM, Schweizer M. In *Saccharomyces cerevisiae*, impaired PRPP synthesis is accompanied by valproate and Li^+ sensitivity. *Biochem Soc Trans* 2005;33:1154–1157.
28. Wang K, Vavassori S, Schweizer LM, Schweizer M. Impaired PRPP-synthesizing capacity compromises cell integrity signalling in *Saccharomyces cerevisiae*. *Microbiology* 2004;150:3327–3339.
29. Zhong G, Wei W, Guan Q, Ma Z, Wei H *et al.* Phosphoribosyl pyrophosphate synthetase, as a suppressor of the sepH mutation in *Aspergillus nidulans*, is required for the proper timing of septation. *Mol Microbiol* 2012;86:894–907.
30. Gupta SK, Maggon KK, Venkitasubramanian TA. Effect of zinc on adenine nucleotide pools in relation to aflatoxin biosynthesis in *Aspergillus parasiticus*. *Appl Environ Microbiol* 1976;32:753–756.
31. Käfer E. Meiotic and mitotic recombination in *Aspergillus* and its chromosomal aberrations. *Adv Genet* 1977;19:33–131.
32. Moreno S, Klar A, Nurse P. Molecular genetic analysis of fission yeast *Schizosaccharomyces pombe*. *Methods Enzymol* 1991;194: 795–823.

33. Wang J, Hu H, Wang S, Shi J, Chen S *et al.* The important role of actinin-like protein (AcnA) in cytokinesis and apical dominance of hyphal cells in *Aspergillus nidulans*. *Microbiology* 2009;155:2714–2725.
34. Wang PM, Choera T, Wiemann P, Pisithkul T, Amador-Noguez D *et al.* TrpE feedback mutants reveal roadblocks and conduits toward increasing secondary metabolism in *Aspergillus fumigatus*. *Fungal Genet Biol* 2016;89:102–113.
35. Zhong GW, Jiang P, Qiao WR, Zhang YW, Wei WF *et al.* Protein phosphatase 2a (PP2A) regulatory subunits ParA and PabA orchestrate septation and conidiation and are essential for PP2A activity in *Aspergillus nidulans*. *Eukaryot Cell* 2014;13:1494–1506.
36. Wang G, Lu L, Zhang CY, Singapuri A, Yuan S. Calmodulin concentrates at the apex of growing hyphae and localizes to the Spitzenkörper in *Aspergillus nidulans*. *Protoplasma* 2006;228:159–166.
37. May GS. The highly divergent beta-tubulins of *Aspergillus nidulans* are functionally interchangeable. *J Cell Biol* 1989;109:2267–2274.
38. Osmani SA, Pu RT, Morris NR. Mitotic induction and maintenance by overexpression of a G2-specific gene that encodes a potential protein kinase. *Cell* 1988;53:237–244.
39. Yu JH, Hamari Z, Han KH, Seo JA, Reyes-Domínguez Y *et al.* Double-joint PCR: a PCR-based molecular tool for gene manipulations in filamentous fungi. *Fungal Genet Biol* 2004;41:973–981.
40. Liu B, Xiang X, Lee YR. The requirement of the LC8 dynein light chain for nuclear migration and septum positioning is temperature dependent in *Aspergillus nidulans*. *Mol Microbiol* 2003;47:291–301.
41. Osmani AH, Oakley BR, Osmani SA. Identification and analysis of essential *Aspergillus nidulans* genes using the heterokaryon rescue technique. *Nat Protoc* 2006;1:2517–2526.
42. Harris SD, Morrell JL, Hamer JE. Identification and characterization of *Aspergillus nidulans* mutants defective in cytokinesis. *Genetics* 1994;136:517–532.
43. Shi J, Chen W, Liu Q, Chen S, Hu H *et al.* Depletion of the MobB and CotA complex in *Aspergillus nidulans* causes defects in polarity maintenance that can be suppressed by the environment stress. *Fungal Genet Biol* 2008;45:1570–1581.
44. Zhang Y, Zheng Q, Sun C, Song J, Gao L *et al.* Palmitoylation of the cysteine residue in the DHHC motif of a palmitoyl transferase mediates $Ca2^{+}$ homeostasis in *Aspergillus*. *PLoS Genet* 2016;12: e1005977.
45. Cai ZD, Chai YF, Zhang CY, Qiao WR, Sang H *et al.* The Gβ-like protein CpcB is required for hyphal growth, conidiophore morphology and pathogenicity in *Aspergillus fumigatus*. *Fungal Genet Biol* 2015;81:120–131.
46. Liu FF, Pu L, Zheng QQ, Zhang YW, Gao RS *et al.* Calcium signaling mediates antifungal activity of triazole drugs in the *Aspergilli*. *Fungal Genet Biol* 2015;81:182–190.
47. Koenigsknecht MJ, Fenlon LA, Downs DM. Phosphoribosylpyrophosphate synthetase (PrsA) variants alter cellular pools of ribose 5-phosphate and influence thiamine synthesis in *Salmonella enterica*. *Microbiology* 2010;156:950–959.
48. Bradford MM. A rapid and sensitive method for the quantitation of microgram quantities of protein utilizing the principle of protein-dye binding. *Anal Biochem* 1976;72:248–254.
49. Song J, Zhai P, Zhang Y, Zhang C, Sang H *et al.* The *Aspergillus fumigatus* damage resistance protein family coordinately regulates ergosterol biosynthesis and azole susceptibility. *MBio* 2016;7:e01919-15.
50. Breakspear A, Momany M. *Aspergillus nidulans* conidiation genes *dewA*, *fluG*, and *stuA* are differentially regulated in early vegetative growth. *Eukaryot Cell* 2007;6:1697–1700.
51. Suh MJ, Fedorova ND, Cagas SE, Hastings S, Fleischmann RD *et al.* Development stage-specific proteomic profiling uncovers small, lineage specific proteins most abundant in the *Aspergillus Fumigatus* conidial proteome. *Proteome Sci* 2012;10:30.
52. Chen P, Gao R, Chen S, Pu L, Li P *et al.* A pericentrin-related protein homolog in *Aspergillus nidulans* plays important roles in nucleus positioning and cell polarity by affecting microtubule organization. *Eukaryot Cell* 2012;11:1520–1530.
53. Hernando Y, Carter AT, Parr A, Hove-Jensen B, Schweizer M. Genetic analysis and enzyme activity suggest the existence of more than one minimal functional unit capable of synthesizing phosphoribosyl pyrophosphate in *Saccharomyces cerevisiae*. *J Biol Chem* 1999;274:12480–12487.
54. Ugbogu EA, Wang K, Schweizer LM, Schweizer M. Metabolic gene products have evolved to interact with the cell wall integrity pathway in *Saccharomyces cerevisiae*. *FEMS Yeast Res* 2016;16:fow092.
55. Nayak T, Szewczyk E, Oakley CE, Osmani A, Ukil L *et al.* A versatile and efficient gene-targeting system for *Aspergillus nidulans*. *Genetics* 2006;172:1557–1566.4

Edited by: A. Alastruey-Izquierdo and V. J. Cid